Proc. Natl. Acad. Sci. USA
Vol. 74, No. 2, pp. 496–500, February 1977
Biochemistry

Mapping of transcription sites of simian virus 40-specific late 16S and 19S mRNA by electron microscopy

(cytoplasmic mRNA/mRNA processing/restriction enzymes/RNA·DNA hybridization)

EVELYNE MAY, JACOB V. MAIZEL, AND NORMAN P. SALZMAN*

National Institutes of Health, Bethesda, Maryland 20014

Communicated by James E. Darnell, Jr., November 12, 1976

ABSTRACT **Simian virus 40 (SV40) late 19S and 16S mRNAs were annealed to complementary regions of partially melted viral double-stranded SV40($L_{Hpa\ II}$) DNA or SV40($L_{Bam\ HI}$) DNA. The RNA·DNA hybrid regions within the DNA molecules were visualized as loops [with SV40($L_{Hpa\ II}$) DNA] or branched molecules [with SV40($L_{Bam\ HI}$) DNA] in the electron microscope. The data confirm the previous localizations of the 3′ and 5′ ends of 16S SV40 mRNA and of the 3′ end of late 19S SV40 mRNA. The 5′ end of the major stable SV40 late 19S mRNA has been positioned at 0.755 map unit. Thus, the sequences of viral DNA from 0.655 to 0.755 map unit, including the replication origin, are not converted into major stable species of late viral mRNA.**

Late in the lytic cycle of simian virus 40 (SV40) there are two distinct classes of viral cytoplasmic RNA that sediment in sucrose gradients at 19 S and 16 S (1, 2). The 19S class includes a low level of 19S early RNA species and a majority of true 19S late RNA species. The early RNA species is complementary to only one of the two strands (the "E" strand), while the late 16S and 19S mRNA species are complementary to the other (the "L" strand) (3, 4). The late RNA species have been mapped by hybridization with SV40 *Hin*d fragments (5, 6). However, by this approach the positioning of the 5′ end of 19S late mRNA was uncertain. The topography of polyoma virus mRNA molecules appears to be very similar (7, 8). Several investigators have suggested that the map position of the 5′ end of early and late mRNA coincides with the site for initiation of DNA synthesis [0.67 map unit (9)] (10, 11), and that this may have some possible biologic significance.

Recently a technique has been developed by Thomas *et al.* (12) in which, under appropriate conditions of hybridization, complementary RNA can hybridize to double-stranded DNA by displacing the part of DNA strand that is identical to this RNA, and the hybrid molecules can be visualized in the electron microscope. Westphal *et al.* (13) have used this procedure to map late adenovirus mRNAs. We have made use of this technique in analyzing hybrids formed between SV40 DNA molecules and SV40 late 19S and 16S mRNA species. By this procedure it has been possible to determine the map positions of both the 5′ and 3′ ends of 16S and 19S mRNAs.

MATERIALS AND METHODS

BSC1 (monkey) cells were infected with plaque-purified wild-type SV40, strain 777, [0.01 plaque-forming unit (PFU) per cell], and virus and viral DNA were purified as described (14). To obtain poly(A)-containing SV40-specific late mRNA, we infected the BSC1 cell culture grown in 150 mm petri dishes 24 hr after seeding (40 PFU per cell). The cultures were labeled for 3 hr at 48 hr after infection with 7 ml of medium containing 250 μCi of [^{3}H]uridine ([5,6-^{3}H]uridine, 50 Ci/mmol, Radiochemical Centre, Amersham) in each petri dish. Poly(A)-containing SV40-specific late mRNA and cellular mRNA were isolated by oligo(dT)-cellulose chromatography according to published procedures (15). Preparative sedimentation to separate the 19S and 16S RNA classes was performed as described (5). The fraction of poly(A)-containing 16S and 19S mRNA that was SV40-specific was determined by hybridization to filters containing SV40 DNA or by liquid hybridization. In the latter procedure, hybrids that were formed were quantitated after Cs_2SO_4 isopycnic centrifugation. Between 25 and 50% of the labeled 16S and 19S mRNA were shown to be virus specific by these procedures.

Linear SV40 [^{14}C]DNA was obtained by cleavage of SV40(I) DNA either by *Bam* HI or by *Hpa* II restriction enzymes (purchased from New England Biolabs). The cleavage products, SV40($L_{Bam\ HI}$) DNA and SV40($L_{Hpa\ II}$) DNA were purified by sedimentation in 5–20% (wt/wt) sucrose gradients (16).

Molecular Hybridization. SV40(L) [^{14}C]DNA (1 μg/ml) and either 19S or 16S SV40 [^{3}H]mRNA (about 0.5 μg/ml) were incubated for 28 hr in hybridization medium. The final composition of this medium was 65% formamide, 2 × SSC, (0.3 M NaCl, 0.03 M Na citrate), 0.1% sodium dodecyl sulfate, and 0.01 M TES [TES = *N*-tris(hydroxymethyl)methyl-2-aminoethane sulfonic acid; Calbiochem, A Grade] pH 7.4. The 100% formamide that was used to prepare hybridization medium was repurified (17).

Electron Microscopy. Immediately after hybridization, the nucleic acids were precipitated with ethanol. The pellet was redissolved in 10 mM Tris, 1 mM EDTA, pH 7.5, for electron microscopy analysis, which was performed as described by Westphal *et al.* (13).

Isopycnic Centrifugation in Cs_2SO_4 was performed in 4.5 ml of a solution of Cs_2SO_4 (ρ_{20} = 1.554 g/cm^3) in 10 mM Tris, 1 mM EDTA, pH 7.4, 1% formamide in a Spinco SW 50.1 rotor at 40,000 rpm for 40 hr at 15°. Fractions of 0.15 ml were collected from the bottom and assayed for total acid-precipitable radioactivity.

Determination of Thermal Midpoint of Melting (t_m) of SV40(L) DNA and SV40 DNA·RNA Hybrids. (*i*) SV40($L_{Hpa\ II}$) [^{14}C]DNA or (*ii*) the corresponding hybrid with late 16S [^{3}H]mRNA dissolved in hybridization medium was exposed at an initial temperature of 35° and the temperature was then progressively raised in 2° increments, allowing 10 min for equilibration at each temperature. At the end of each 10-min period, an aliquot of 40 μl was taken to determine the acid-precipitable cpm either after S_1 nuclease treatment of the SV40($L_{Hpa\ II}$) DNA (18) or after RNase treatment of the hybrid. (Pancreatic RNase was treated at 80° for 15 min prior to use. Digestion was with 20 μg/ml in 2 × SCC for 30 min at room temperature.) The results are given as the percentage of the total radioactivity of the DNA or hybrid that remains acid-precipitable, and this is plotted as a function of the temperature.

Abbreviations: SV40, simian virus 40; t_m, thermal midpoint of melting.

* To whom reprint requests should be addressed: National Institutes of Health, National Institute of Allergy and Infectious Diseases, Laboratory of Biology of Viruses, Bethesda, Maryland 20014.

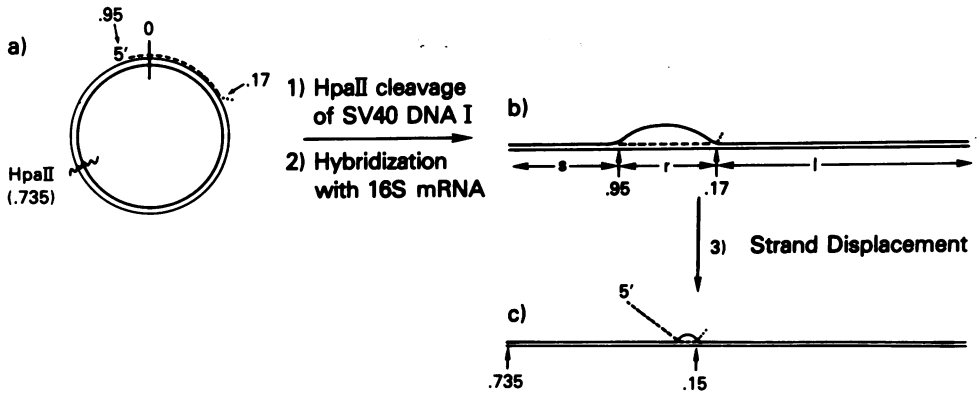

FIG. 1. Schemes for hybridization of SV40($L_{Hpa\ II}$) DNA with 16S mRNA. (a) Scheme indicating the region of viral genome that corresponds to the stable SV40 late 16S mRNA [the poly(A) tract represented by the dotted line is shown at the 3′ end of mRNA]. (b) Hybrid molecule before branch migration. (c) Hybrid molecules after branch migration. Hybrid molecules (b and c) contain a short DNA duplex segment, an R-loop, and a large duplex segment, which are designated respectively *s*, *r*, and *l*. While branch migration forms an RNA tail at each fork, there is very limited displacement of mRNA at the 3′ end, but extensive displacement of the mRNA molecule at the 5′ end. Solid, dashed, and dotted lines represent, respectively, DNA strand, RNA, and poly(A) tract.

The temperature at which this percentage corresponds to 50% is taken as the t_m.

RESULTS

Formation and Properties of Hybrids. SV40($L_{Hpa\ II}$) [^{14}C]DNA (1 μg/ml) and SV40 specific late 16S mRNA that was [^{3}H]uridine-labeled and contained poly(A) (0.5 μg/ml) were incubated for 28 hr at 50° in hybridization medium. The hybridization products were precipitated with ethanol, then redissolved in 2 × SSC and divided in two portions. One portion was directly analyzed by isopycnic centrifugation in Cs_2SO_4, while the other portion was centrifuged in parallel after treatment with pancreatic RNase (20 μg/ml of RNase in 2 × SSC for 30 min at room temperature). Without RNase treatment 50% of the ^{3}H radioactivity in RNA banded at the position of free RNA, while the other 50% was in the region where RNA·DNA hybrids are expected and banded at a density one fraction heavier than the peak of the [^{14}C]DNA radioactivity. After RNase treatment the peak of free [^{3}H]RNA disappeared, but as much as 80% of [^{3}H]RNA that was originally detected in the hybrid region was recovered. The resistance of the DNA·RNA hybrids to RNase treatment indicates that the hybrid is in close register. Twenty-five percent of the radioactivity of the 16S RNA preparation was found to hybridize to excess denatured SV40 DNA on filters [the hybridization was performed in 50% formamide (2)]. Because 50% of the 16S [^{3}H]RNA was found in the RNA·DNA hybrid region in Cs_2SO_4, we can conclude that all SV40 specific mRNA present in the 16S RNA preparation hybridized with SV40($L_{Hpa\ II}$) DNA. Identical results were obtained with SV40($L_{Bam\ HI}$) DNA. The t_m in hybridization medium of SV40($L_{Hpa\ II}$) DNA and of the corresponding hybrid with late 16S mRNA were, respectively, 53.5° and 58.5°. These results showed that *in hybridization medium* the DNA·RNA hybrid has a greater thermodynamic stability than the DNA duplex.

Electron Microscopic Analysis of Hybrids of SV40($L_{Hpa\ II}$) DNA and Poly(A)-Containing Late mRNA. As noted previously, by using hybridization of viral mRNA to specific fragments of the viral genome, the 16S late mRNA has been positioned relative to the SV40 genome with the 5′ end at 0.95 map unit and the 3′ end at 0.17 map unit. In Fig. 1 we have represented schematically the structures that would be generated when this 16S RNA is hybridized to SV40 DNA after the DNA has been converted to a linear molecule by cleavage with *Hpa* II at 0.735 map unit (19). The expected conformation of the hybrid molecules should be that shown schematically in Fig. 1b. When the hybrids were examined by electron microscopy, we observed molecules with this structure (Fig. 2a). The predominant hybrid forms, however, are not these, but seem to arise by partial displacement of the hybridized RNA. Such structures are represented schematically in Fig. 1c, and such

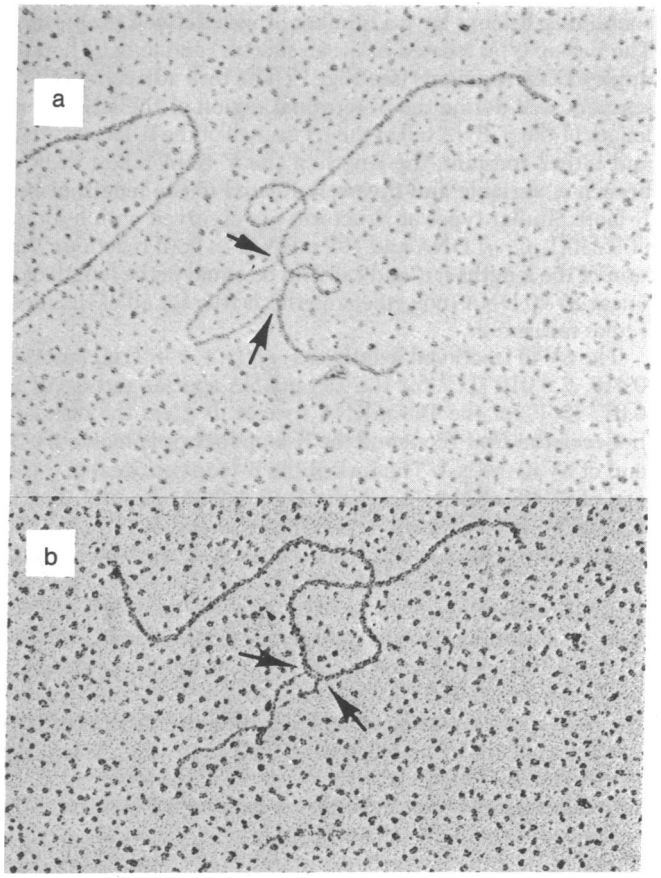

FIG. 2. Electron micrographs of hybrid molecules formed between SV40($L_{Hpa\ II}$) DNA and SV40 late mRNA. The two arrows in each panel indicate the junction of segments *r* and *l* and of *r* and *s*. In each panel there is a short, single-stranded RNA segment that is at the *r*, *l* junction. In panel b, single-stranded RNA is also seen at the *r*, *s* junction. The regions *l*, *r*, and *s* are defined in Fig. 1.

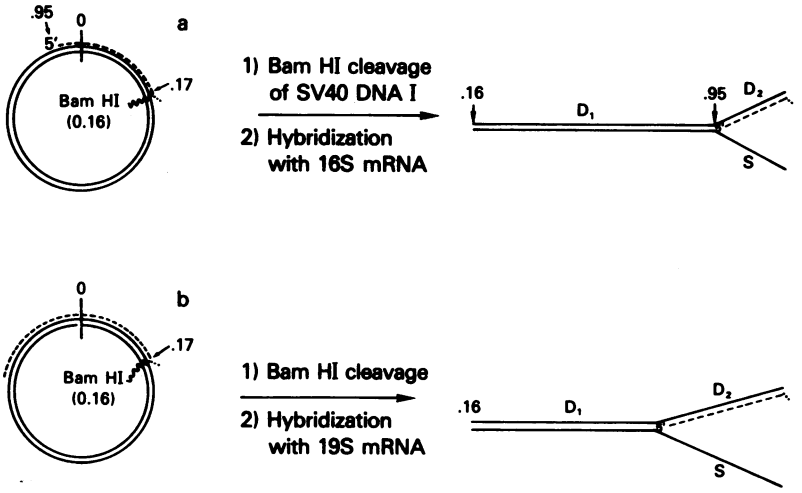

FIG. 3. Schemes for hybridization of SV40($L_{Bam\ HI}$) DNA with 16S or 19S mRNA. (Left) Schemes indicating the regions of the viral genome that correspond to stable SV40 late 16S and 19S mRNA [the poly(A) tract is represented at the 3′ end of mRNA]. (Right) Hybrid molecules: the hybrid molecules are Y-shaped and contain a homoduplex DNA segment (D_1), a heteroduplex DNA·RNA segment (D_2), and a single-stranded DNA segment (S) extending from the branched point. Solid, dashed, and dotted lines represent, respectively, DNA strand, RNA, and poly(A) tract.

molecules are illustrated in Fig. 2b. RNase treatment at the completion of the hybridization reaction solubilizes only 20% of the label in the hybrid. Because most of the hybrids showed extensive regions containing unhybridized RNA (see Fig. 2b), it follows that strand displacement occurred during the preparation of the sample for electron microscopy. The molecules containing R-loops have a number of well defined properties. The R-loop (r) is located between short (s) and long (l) homoduplex DNA segments (see Fig. 1). The fork adjacent to the l segment will define the 3′-terminal region of the RNA. The length of the 3′ RNA tail at the r, l branch of the R-loop is small and rather constant; the length of the 5′ RNA tail at the r, s branch is variable and inversely related to the length of the R-loop. Similar types of structures are observed with hybrids of SV40($L_{Hpa\ II}$) DNA and 19S mRNA. In both reactions, the sum of the lengths s, r, and l should be equal to the length of a linear SV40 DNA molecule, and this is true for all of the molecules measured.

The SV40 fractional length $(s + r)/(s + r + l)$ is constant, 0.418 ± 0.019 [17]† for the 19S mRNA species and 0.419 ± 0.017 [26]† for the 16S mRNA species. It gives the distance between the *Hpa* II cut and the R-loop fork proximal to the 3′ end of SV40 mRNA. The fork of the R-loop proximal to the 3′ end of SV40 mRNA is located at 0.15 ± 0.02 map unit. This is calculated from the ratio $(s + r)/(s + r + l) + 1$–0.735. The lengths of the RNA tail at the r, l branch of the R-loop were, respectively, 0.035 ± 0.026 [6]† and 0.040 ± 0.016 [31]† for poly(A)-containing SV40 specific late 19S and 16S mRNA species. Assuming that the poly(A) tail at the 3′ end of mRNA contains 100 adenylate residues (20), its length corresponds to approximately 0.02 SV40 fractional length. Thus, the 3′ end of the virus-specific portion of both late 19S and 16S SV40 mRNA species appears to be located at 0.17 map unit. While the preservation of secondary structure in single-stranded RNA introduces a large error in length measurements, because of the small size of the RNA tail at the r, l branch, the location of the 3′ end of the mRNA can be accurately determined. However, we have not been able to position the 5′ end of the 16S or 19S mRNA by measurements of the single-stranded RNA tail at the r, s branch, but instead, we have relied on cleavage of SV40 DNA by *Bam* HI for this determination (see following section).

Hybrids of SV40($L_{Bam\ HI}$) DNA and Poly(A)-Containing SV40 Late mRNA. *Bam* HI cleaves the SV40 genome at 0.16 map unit (21), which is at or near the site coding for the 3′ end of late SV40 mRNA. Fig. 3 shows a diagrammatic representation of the branched hybrid molecules that are expected when this linear DNA is hybridized with viral mRNA, and Fig. 4 illustrates the molecules that are observed by electron microscopy. They consist of three segments, D_1, D_2, and S, extending

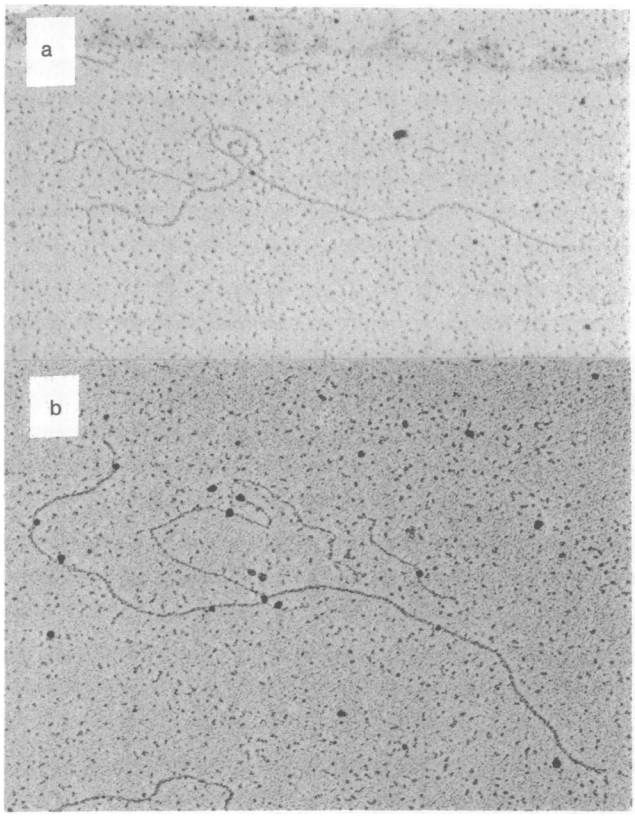

FIG. 4. Electron micrographs of hybrid molecules formed between SV40($L_{Bam\ HI}$) DNA and SV40 late mRNA. Hybrids formed with 16S mRNA (a) or with 19S late mRNA (b).

† Each value represents the mean ±SD; the number in brackets is the number of hybrid molecules that were measured.

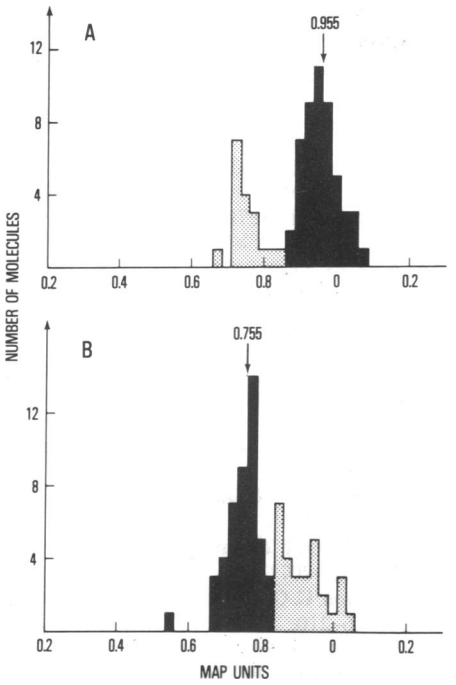

FIG. 5. Histograms of SV40 late mRNA in relation to the map location of their 5′ end. Preparation of 16S mRNA (A); of 19S mRNA (B). After hybridization of SV40($L_{Bam\ HI}$) with either 16S or 19S mRNA, the position of the fork in Y-shaped molecules was calculated as noted in the text. The linear duplex DNA molecule was cleaved by the restriction enzyme *Bam* HI at 0.16 map unit.

from the branched point. The segments D_1 and D_2 are duplex, while S is single-stranded. The contour lengths of these segments have the following relationship: $D_1 > D_2$ or S, and D_2 and S are similar in length in a single molecule. Thus, D_2 corresponds to the heteroduplex region of the hybrid molecule while S is the single-stranded DNA that has been displaced by the RNA molecule. Electron microscopy reveals that only 1–2% of DNA molecules are branched. This percentage is lower than we would predict from the data obtained by Cs_2SO_4 isopycnic centrifugation analysis of RNA·DNA hybrids. The low frequency of hybrid molecules probably results from an extensive branch migration that occurs during the spreading of the molecules. The difference in stability of hybrid molecules found with SV40 DNA generated with *Hpa* II or with *Bam* HI may result from the presence around or adjacent to 0.15 map unit of a region whose local structure stabilizes the hybrid. When the DNA is cut in this region (as with *Bam* HI), it is no longer possible to stabilize an RNA·DNA hybrid when strand displacement occurs. The hybrids that are formed with mRNA and SV40($L_{Hpa\ II}$) DNA demonstrate the stability of hybrids in the region of the DNA molecule at 0.15 map unit. The ratio $D_2/(D_1 + D_2)$ gives the fractional length of SV40 mRNA present in the hybrid. The 5′-terminus of the different SV40 mRNAs is given by the following relation: 5′ end location (map units) = $1.16 - [D_2/(D_1 + D_2)]$. These values are plotted as a histogram (Fig. 5).

The data for the preparations of 16S and 19S late mRNA (Fig. 5A and B) show a cross contamination of each 16S and 19S mRNA species with the other. However, for each preparation there is clearly a predominant homogeneous subgroup corresponding to the 5′ end of 16S late mRNA molecules (from 0.860 to 0.060 map units, panel A) and of 19S late mRNA molecules (from 0.660 to 0.835 map units, panel B). From this grouping one can compute the map location of the 5′ terminus of the

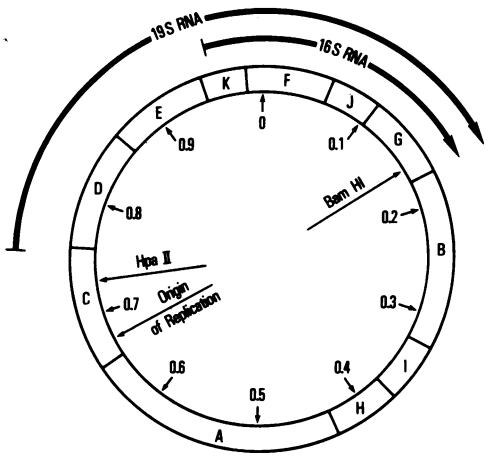

FIG. 6. Mapping of the major, stable SV40 late mRNA species. The poly(A) tracts at the 3′ end of mRNA are not represented.

SV40 16S and 19S late mRNA species that contain poly(A), expressed as mean values (map units) ±SD [the number of molecules in the subgroup are given in brackets]. The 5′-end location of 16S late mRNA is 0.955 ± 0.045 [50]; the 5′-end location of 19S late mRNA is 0.755 ± 0.040 [45]. In the histogram of the preparation of 19S late mRNA (Fig. 5B) we cannot exclude the presence of a minor species of 19S mRNA which would correspond to a 5′-end location at about 0.85 map unit.

DISCUSSION

By electron microscopic examination of hybrid molecules formed between SV40($L_{Hpa\ II}$) DNA and SV40 late mRNAs, we have been able to position the 3′ end of both 16S and 19S late mRNA at 0.17 map unit. These hybrids contain an R-loop in which one branch is always located at 0.15 map unit. This is the site at which the hybrid is most stable. Dhar *et al.* have observed that a preferred promoter site for *E. coli* polymerase on the SV40 genome is located at 0.15 map unit (22). This site (in the *Hin*d G fragment) also contains one of the three regions in which DNA is capable of reacting as though it had single-stranded properties (23). The structural feature of this region, which has a high content of adenine and thymine (22), may promote particularly favorable energetics of hybridization to RNA.

Electron microscopic examination of hybrid molecules formed between SV40($L_{Bam\ HI}$) DNA and SV40 late mRNAs has enabled us to position the 5′ end of SV40 late mRNAs owing to the cleavage site (at 0.16 map unit) of *Bam* HI. This was possible even though only a small percentage of the DNA molecules examined by electron microscopy were actually DNA·RNA hybrids. It is clear that the restriction enzyme cleavage site is an important determinant of the stability of RNA·DNA hybrid, and this is most likely due to extensive branch migration during the spreading. We have found that the 5′ end of 16S and 19S mRNA species are located at about 0.955 and 0.755 map unit, respectively. The above data are summarized in Fig. 6. Our data confirm the previous localizations of 3′ and 5′ ends of 16S SV40 mRNA and of the 3′ end of late 19S SV40 mRNA (5, 6). This result demonstrates that those hybrid molecules that are observed by electron microscopy are representative of the whole population of hybrid molecules. The localization of the 5′ ends of SV40 late 19S mRNA at 0.755 map unit places it 0.085 map unit away from the replication origin, which is located at 0.67 map unit (9).

Previous results suggested that SV40 late mRNAs were complementary to the region of SV40 DNA late strand extending from 0.65 to 0.17 map unit (24). The method used in that work (RNA-excess hybridization) gave the furthest extent of the late region, including major and minor species of late mRNA.

The SV40 mRNA species shown in fig. 6 are the major stable 19S and 16S late mRNA species. The presence of minor species of late mRNA would not be observed by this procedure. Dhar *et al.* (10, 25) detected a species of SV40 19S late mRNA whose 5′ end is specified by the nucleotide sequence of a fragment that contains the origin of DNA replication. In these studies, there was a preselection of RNA molecules that contain sequences homologous to the viral genome at 0.63 to 0.70 map unit. The species preselected might represent a minor late mRNA species or they could be unprocessed late mRNA.

The present positioning of the 5′ end of the 19S mRNA at 0.755 map unit is in good agreement with our current understanding of the viral gene products that are coded for by late mRNA. Shenk *et al.* (19) have shown that one of the three regions that can be deleted without affecting the viability of the virus occurs between 0.68 and 0.74 map unit. Three late viral gene products, VP1 (molecular weight, 41,000–49,000), VP2 (30,000–34,000), and VP3 (22,000–24,000) (26), are coded for by that part of the viral genome from 0.755 to 0.17. The region from 0.95 to 0.17 corresponds to the late 16S mRNA and it specifies the synthesis of VP1 (5, 6, 27). The part of the genome coding for VP3 is adjacent to the VP1 region (Cole, Landers, and Berg, personal communication) and, based on the position of temperature-sensitive mutants of VP1 and VP3 (28) and fingerprints of the two gene products (29), there is no evidence for genetic overlapping. Both Fey and Hirt and Cole, Landers, and Berg (personal communications) have also shown that most or all of the sequences coding for VP3 are included in those sequences that specify VP2. Thus, the portion of stable SV40 late 19S mRNA that is not shared with the late 16S mRNA species, which is equivalent to 20% of the viral genome (from 0.755 to 0.955 map unit) or about 300,000–340,000 daltons of single-stranded DNA, is sufficient to specify VP2 and VP3.

We acknowledge valuable discussions with Dr. Pierre May and thank him for his invaluable assistance in the preparation of this manuscript. We are indebted to Mrs. M. Sullivan for her skillful preparation of the electron micrographs.

1. Weinberg, R. A., Warnaar, S. O. & Winocour, E. (1972) *J. Virol.* **10,** 193–201.
2. May, E., May, P. & Weil, R. (1973) *Proc. Natl. Acad. Sci. USA* **70,** 1654–1658.
3. Khoury, G., Martin, M. A., Lee, T. N. H., Danna, K. J. & Nathans, D. (1973) *J. Mol. Biol.* **78,** 377–389.
4. Sambrook, J., Sharp, P. A. & Keller, W. (1972) *J. Mol. Biol.* **70,** 57–71.
5. May, E., Kopecka, H. & May, P. (1975) *Nucleic Acids Res.* **2,** 1995–2005.
6. Khoury, G., Carter, B. J., Ferdinand, F. J., Howley, P. M., Brown, M. & Martin, M. A. (1976) *J. Virol.* **17,** 832–840.
7. Kamen, R. & Shure, H. (1976) *Cell* **7,** 361–371.
8. Türler, H., Salomon, C., Allet, B. & Weil, R. (1976) *Proc. Natl. Acad. Sci. USA* **73,** 1480–1484.
9. Fareed, G. C., Garon, C. F. & Salzman, N. P. (1972) *J. Virol.* **10,** 484–491.
10. Dhar, R., Subramanian, K. N., Zain, B. S., Levine, A., Patch, C. & Weissman, S. M. (1975) "Les Colloques de l'Institut National de la Santé et de la Recherche Médicale," *INSERM Colloq.* **47,** 25–32.
11. Tegtmeyer, P., Schwartz, M., Collins, J. K. & Rundell, K. (1975) *J. Virol.* **16,** 168–178.
12. Thomas, M., White, R. L. & Davis, R. W. (1976) *Proc. Natl. Acad. Sci. USA* **73,** 2294–2298.
13. Westphal, H., Meyer, J. & Maizel, J. V. (1976) *Proc. Natl. Acad. Sci. USA* **73,** 2069–2071.
14. Lebowitz, J., Caron, C. G., Chen, M. C. Y. & Salzman, N. P. (1976) *J. Virol.* **18,** 205–210.
15. Rosenthal, L. J. (1976) *Nucleic Acids Res.* **3,** 661–676.
16. Thoren, M. M., Sebring, E. D. & Salzman, N. P. (1972) *J. Virol.* **10,** 462–468.
17. Tibbets, C., Johansson, K. & Philipson, L. (1973) *J. Virol.* **12,** 218–225.
18. Gunther, M. & May, P. (1976) *J. Virol.* **20,** 86–95.
19. Shenk, T. E., Carbon, J. & Berg, P. (1976) *J. Virol.* **18,** 664–671.
20. Brawerman, G. & Diez, J. (1975) *Cell* **5,** 271–280.
21. Kevner, G. & Kelly, T. J. (1976) *Proc. Natl. Acad. Sci. USA* **73,** 1102–1106.
22. Dhar, R., Zain, S., Weissman, S. M., Pan, J. & Subramanian, K. N. (1974) *Proc. Natl. Acad. Sci. USA* **71,** 371–375.
23. Chen, M., Lebowitz, J. & Salzman, N. P. (1976) *J. Virol.* **18,** 211–217.
24. Khoury, G., Howley, P., Nathans, D. & Martin, M. A. (1975) *J. Virol.* **15,** 433–437.
25. Dhar, R., Subramanian, K. N., Pan, J. & Weissman, S. M. (1976) *J. Biol. Chem.* **252,** 368.
26. Lake, R. S., Barban, S. & Salzman, N. P. (1973) *Biochem. Biophys. Res. Commun.* **54,** 640–647.
27. Prives, C. L., Aviv, H., Gilboa, E., Revel, M. & Winocour, E. (1974) *Cold Spring Harbor Symp. Quant. Biol.* **39,** 309–316.
28. Lai, C. J. & Nathans, D. (1975) *Virology* **66,** 70–81.
29. Zweig, M., Barban, S. & Salzman, N. P. (1976) *J. Virol.* **17,** 916–923.